processes

MDPI

Article

Study on the Variation Laws and Fractal Characteristics of Acoustic Emission during Coal Spontaneous Combustion

Jueli Yin [1], Linchao Shi [2], Zhen Liu [1,*], Wei Lu [2], Xingsong Pan [3], Zedong Zhuang [2], Lei Jiao [4] and Biao Kong [2,*]

[1] College of Finance and Economics, Shandong University of Science and Technology, Taian 271000, China
[2] College of Safety and Environmental Engineering, Shandong University of Science and Technology, Qingdao 266590, China
[3] Dongtan Coal Mine, Yanzhou Coal Mining Company Ltd., Jining 272000, China
[4] Qingdao Sinotrans Logistics Co., Ltd., Qingdao 266000, China
* Correspondence: jinanlanchuan@163.com (Z.L.); kongbiao8807@163.com (B.K.)

Abstract: Acoustic emission (AE) technology has the advantage of online localization to study the change laws of AE in the process of coal spontaneous combustion and to reveal the generation mechanisms of AE signal during the process of heating and rupture of coal body from a microscopic perspective. This paper first constructs a large-scale coal spontaneous combustion AE test system and conducts experimental tests on the AE signal in the process of coal spontaneous combustion. The results show that with the increase of temperature in the process of coal spontaneous combustion, the AE signal shows a trend of increasing fluctuations. Low-temperature nitrogen adsorption experiments studied the pore structure of coal spontaneous combustion, and the results showed a correspondence between the development of pores and the temperature of coal spontaneous combustion. Further, through the analysis of the evolution of the pore structure of coal through Fourier transform and fractal theory, it is found that the high-frequency main frequency AE signal and average frequency are continuously enhanced with the increase of temperature. The fractal dimension of the pore structure and the fractal dimension of the AE count of the coal body first rise and then decline. The mechanism of coal spontaneous combustion AE of coal is revealed, and the pore development caused by thermal stress when coal heats up is the main source of AE signal generation. The research in this paper is of great significance for applying AE technology to detect the position of coal spontaneous combustion.

Keywords: coal spontaneous combustion; thermal rupture; AE; time frequency; fractal

Citation: Yin, J.; Shi, L.; Liu, Z.; Lu, W.; Pan, X.; Zhuang, Z.; Jiao, L.; Kong, B. Study on the Variation Laws and Fractal Characteristics of Acoustic Emission during Coal Spontaneous Combustion. *Processes* **2023**, *11*, 786. https://doi.org/10.3390/pr11030786

Academic Editors: Feng Du, Aitao Zhou and Bo Li

Received: 7 February 2023
Revised: 1 March 2023
Accepted: 2 March 2023
Published: 7 March 2023

1. Introduction

Coal spontaneous combustion is serious in China, resulting in a massive waste of resources. Coal spontaneous combustion monitoring and early warning technologies mainly include temperature detection methods, infrared detection methods, gas detection methods, magnetic force detection methods, transient electromagnetic methods, resistivity detection methods, etc. [1]. In recent years, bundle tube monitoring, distributed optical fiber temperature measurement, and wireless temporary network temperature measurement technology have also been widely used in coal spontaneous combustion disaster monitoring and early warning. However, these monitoring and early warning methods still have certain drawbacks [2]. Bundle tube monitoring temperature measurement and distributed fiber optic temperature measurement are subject to large environmental factors in practical applications, and the data is easily distorted in complex mine environments [3–5]. Wireless self-assembling network temperature measurement systems will not be affected by problems such as pipelines being damaged. Due to the complexity of the mining area environment, the wireless signal transmission is unstable, and difficult to achieve efficient monitoring [6].

AE detection technology based on coal heating and the heating process fracture to generate the elastic waves phenomenon for monitoring and early warning of coal spontaneous combustion is a non-contact, non-destructive testing technology. In recent years, many scholars have linked AE with the prediction of coal body thermodynamic disasters, realized non-contact detection of coal body thermodynamic disasters in coal mines through AE technology, and provided precursor information of coal body thermodynamic disasters through the characteristics of AE activities.

At present, scholars at home and abroad have conducted a large number of studies on the AE law of coal rock. Ganne et al. studied the AE characteristics of hard and brittle rocks and established the relationship between micro-rupture and AE parameters [7]. Ishida et al. studied the distribution characteristics of AE sources during misalignment tests [8]. Han et al. investigated the AE characteristics of different coal samples during the process under uniaxial compression and found that there were significant differences in the AE characteristics of coal with different strengths during the compression process [9]. Kong et al. [10–12] studied the AE nonlinear and fractal characteristics of AE under multiple heating and loading damage conditions of coal rocks. Chen, under laboratory conditions, analyzed the acoustic emission count, dissipation energy, and fracturing point distribution of different deformation stages of coal [13]. Zhang studied the AE signal pattern and multiple fractal characteristics of coal deformation damage under different conditions [14]. The AE response characteristics of anthracite coal were studied through ultrasonic experiments [15]. In uniaxial compression experiments, it was found that when the density was higher than a specific value, the wave velocity of the coal sample increased with the increase of density, and the distribution of AE events over time was approximately normally distributed. Li et al. studied the AE characteristics of different coal-thick coal-rock assemblies during the rupture process and found that the peak count of AE was negatively correlated with coal thickness, and the cumulative count of AE was positively correlated with coal thickness [16].

Scholars at home and abroad have also done a lot of research on the changing laws of the pore structure of coal bodies. They studied the pore structure and fractal characteristics of different coals and found that the pores and fractures in coal become simpler and simpler during the crushing of coal samples, which is more favorable for gas storage and transport [17,18]. Li et al. conducted uniaxial compression tests on coal samples with prefabricated cracks at different angles and found that the AE response showed significantly different characteristics at different stages [19]. Zhao et al. analyzed the influence of the question on the transformation of coal pore structure and concluded that the higher the temperature, the greater the pore fractal dimension of the large pore in the coal [20]. Yi et al. analyzed the pore evolution of hydrochloric acid-treated coal samples by the low-temperature gas adsorption (LTGA) method and found that fractal dimension D2 was significantly positively correlated with ash content and increased with the increase of hydrochloric acid concentration [21]. Xu et al. studied the effect of microwave-assisted oxidant stimulation based on low-temperature nitrogen adsorption on the pore structure and fractal characteristics of bituminous coal. They found that microwave-assisted oxidation expanded the internal pore space and promoted pore expansion [22].

The above studies show that during the heating process, the structure of the coal body will change significantly with the increase in temperature. At different temperatures, it will show different characteristics, mainly changes in the structure of pore fractures [23–30]. There are many similarities between the damage change of coal in the process of heating and the damage change at the time of load deformation and rupture, and both processes are accompanied by the generation of AE signal, which provides conditions for the monitoring and early warning of hidden fire sources under coal mines through AE technology. The fractal theory is primarily used in the study of uniaxial compression and thermal rupture damage of coal rocks, and in recent years, the research on AE of coal bodies has gradually increased, but these studies have less analysis of the law and generation mechanism of coal spontaneous combustion AE signal. The passive monitoring technology of AE can realize

the source finding and locating of underground fire sources and improve the efficiency of coal spontaneous combustion monitoring and early warning, and there is less research on the monitoring and early warning technology of the whole process of coal spontaneous combustion, which needs further research exploration in theory.

Based on the advantages of the acoustic method of temperature measurement, the application of AE technology for coal spontaneous combustion monitoring to achieve underground hidden fire source early warning has a good prospect. In contrast, the characteristics of AE signal changes during coal warming have not been studied in depth, and the mechanism of AE generation during coal warming has not been revealed. Based on this, this paper constructs a large-scale coal spontaneous combustion AE test system and a low-temperature nitrogen adsorption experimental platform, studies the thermal rupture and AE signal laws during the spontaneous combustion and heating of coal, analyzes the AE count and energy changes during the coal spontaneous combustion, reveals the temporal and frequency characteristics of AE signal by using Fourier transform, analyzes the fractal characteristics of low-temperature nitrogen adsorption and AE counts by fractal theory, and discusses the mechanism of the pores generated by thermal damage of coal bodies during coal spontaneous combustion heating process as the source of AE signal. The counting, energy, and spectral laws of the AE signal in the coal spontaneous combustion process are studied, and the fractal laws of BET of coal after different temperature treatments are analyzed. The nonlinear characteristics between AE and the pore structure of coal are revealed. This study lays a foundation for further exploring the heating coal body's AE signal generation mechanism and improving the monitoring and early warning of the spontaneous combustion fire of the AE signal coal.

2. Experimental System and Experimental Protocol

2.1. Large-Scale Coal Spontaneous Combustion AE Experiment

2.1.1. Preparation and Analysis of Coal Samples

In this paper, the main objective is to investigate the characteristic patterns and differences of AE signals generated at different temperature stages during the warming and combustion of coal. In addition, we studied the mechanism of AE generation, which provides a theoretical basis for AE signal inversion of temperature and monitoring of coal spontaneous combustion. Based on this, bituminous coal (DT) sample from the Dongtan coal mine in Shandong, China, was selected for the large-scale coal spontaneous combustion AE experiment, with a weight of 3 tons. In order to ensure that the coal pile has better heat storage conditions, some of the coal blocks were crushed below 30 mm. The volatile fraction (V_{daf}) and five elemental contents of C, H, O, N, and S of DT coal samples at room temperature were analyzed by a 5E-MAG6700 fully automatic industrial analyzer, and the volatile fraction and elemental composition of coal samples were determined according to the national standard GB/T 212-2008 as shown in Table 1.

Table 1. Volatile and elemental analysis of coal samples.

DT Coal Sample (Room Temperature)					
V_{daf}, wt%	C_{daf}/%	H_{daf}/%	O_{daf}/%	N_{daf}/%	$S_{t.d}$/%
40.96	81.16	6.11	0.33	1.16	11.20

2.1.2. Experimental System

The large-scale coal spontaneous combustion AE test system is mainly composed of a furnace body, an AE monitoring system, a hot air input system, and a thermocouple temperature measurement system. Among them, the furnace body is cylindrical, the surface is a metal shell, and the interior is composed of a refractory brick layer, polyurethane thermal insulation layer, water sandwich layer, etc. The hot air input system consists of an air pump, a heating tank, a metal hose, and a temperature control box. The thermocouple temperature measurement system is composed of K type thermocouple and a temperature

recorder. The AE monitoring system is composed of an AE probe, AE host, preamplifier, and waveguide rod, where the AE sensor operates in the frequency range of 10 KHz–2 MHz. Figure 1 shows a large-scale coal spontaneous combustion AE test system diagram.

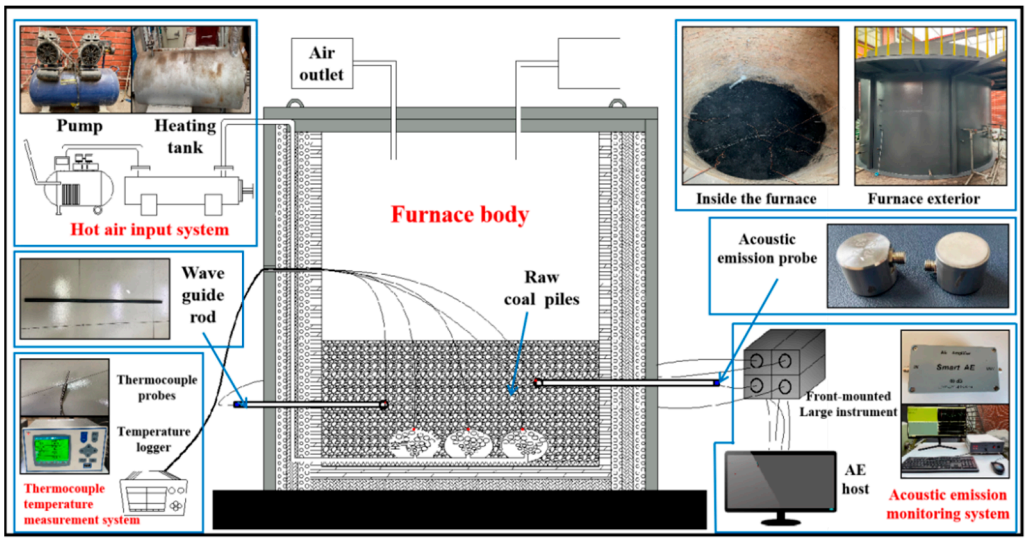

Figure 1. Large-scale coal spontaneous combustion AE test system diagram.

2.1.3. Experimental Methods and Steps

The large-scale coal spontaneous combustion AE experiment is divided into three steps:

(1) First, the 4 waveguide rods are extended into the furnace through the pores, and the horizontal distance of each waveguide rod from the nearest vent is 10 cm, 20 cm, 20 cm, and 40 cm. The distance from the bottom of the furnace is 37 cm, 35 cm, 15 cm, and 35 cm. The 4 waveguide rods are defined as channels 1–4, and 1 thermocouple probe is arranged at the top of the 4 waveguide rods and 3 outlets to measure the temperature of the surrounding coal body.

(2) After the arrangement is completed, 3 tons of raw coal are poured into the inside of the furnace body, the top cover of the furnace body is covered, and the top cover is sealed with glue, the ventilation hole is reserved, and the air is pressed into the heating tank by the air pump, and the heated air enters the bottom of the furnace body through the metal hose, flows out through 3 outlets, and continuously heats the coal body inside the furnace body, of which the ventilation pipe is located in the middle of the furnace body close to the bottom of the furnace body.

(3) The top of the waveguide rod extends into the inside of the furnace, and the tail end is connected to the AE probe. The sound wave can be transmitted to the AE probe by low loss through the waveguide rod to be monitored and recorded, and the waveform is finally saved to the AE host.

The noise reduction process is performed before the experiment, and the threshold value is set in advance. In order to avoid noise triggering, the threshold value is set relatively high, and the signal below the threshold value is not processed in any way. If the waveform below the threshold value is also found to be valuable, then the relatively weak signal can be analyzed by resetting the threshold value. During this experiment, we try to keep it quiet to avoid generating too much noise, and the threshold is set to 5 mV. When extracting the data, the part of the signal is masked out by the set threshold value. The preamplifier used in this experiment has a multiple of 40 dB and a sampling frequency of 200 kHz. During the heating process, the thermocouple temperature measurement system continuously records the internal temperature of the furnace body and saves the temperature data to the temperature recorder.

2.2. Coal Sample Low-Temperature Nitrogen Adsorption Experiment with Different Temperature Treatment

During the experiment, after transporting the packaged fresh coal samples to the laboratory, the whole coal sample is knocked out with a geological hammer to take a small coal sample with a length of no more than 1 cm in width and height. The small coal samples were put into a programmed heating furnace and treated with a temperature constant temperature of 30 °C, 100 °C, 200 °C and 300 °C for 3 h and cooled freely. For 4 groups of experimental samples, the automatic specific surface area and porosity analyzer were selected for low-temperature nitrogen adsorption experiments. The coal samples treated at different temperatures were screened, and the pulverized coal with specifications 40–80 was obtained, and then the sieved pulverized coal was put into the dry sample tube for degassing because the process of thermal expansion and rupture of the coal rock mass was irreversible [31,32]. Thus, in order to avoid excessive deregulation temperature to change the coal pore fracture structure, the degassing temperature of the coal sample was set below the treatment temperature. The pore fracture structure of the coal body would not be affected at this time. Since degassing requires the removal of moisture and air, it is difficult to remove moisture at room temperature, so the samples treated at 30 °C are degassed in a vacuum for 48 h at 30 °C, while the samples treated at 100 °C, 200 °C and 300 °C are degassed at 100 °C vacuum for 12 h.

3. Study on the Thermal Damage Law of Coal Body during Spontaneous Combustion and Heating Process of Coal

3.1. AE Counting and Energy Analysis during Spontaneous Combustion and Heating of Coal

Through the two aspects of AE characteristic parameters and spectrum, the data obtained by the large-scale coal spontaneous combustion AE test system are analyzed. The characteristic parameters are selected for counting and energy. The current research on coal spontaneous combustion shows that the occurrence and development of coal spontaneous combustion have stage characteristics in different temperature bands [33]. Based on this, the experimental process in Figures 2 and 3 is divided according to the temperature stages, and the change law of the AE signal is analyzed. The third stage of the sample has entered the high-temperature state after rapid warming, and the subsequent warming is slower [10]. Figure 2 shows the law of the change of AE counts with time during the heating process of coal.

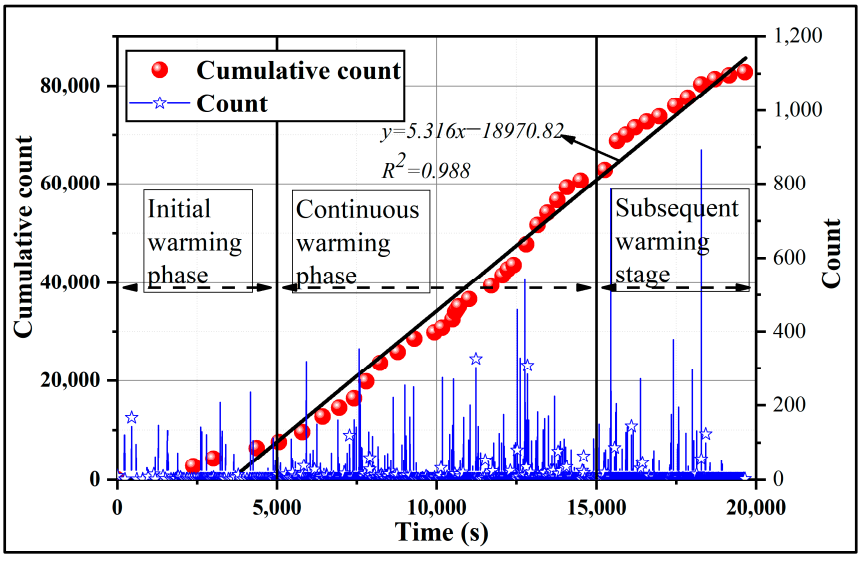

Figure 2. AE count and cumulative count plot.

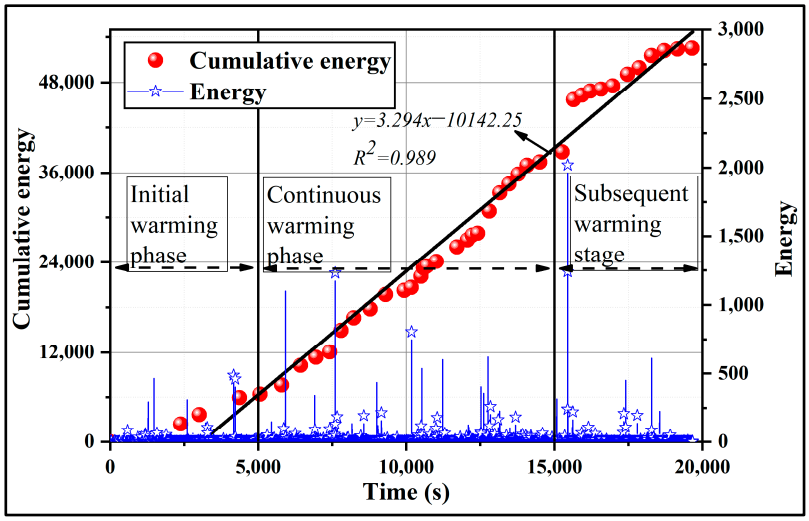

Figure 3. AE energy and cumulative energy map.

As can be obtained from Figure 2, with the progress of the experiment, there is a gradual increase in the AE count in the initial heating stage of 0~5000 s due to the low temperature. The coal body has not obtained enough energy, and the thermal stress is not enough to destroy the coal body itself. Only more fine cracks are generated. Therefore, the integrity of the coal sample is better, and the AE signal is less. In the continuous heating stage of 5000~15,000 s, the coal body has a higher temperature. With the increase in temperature, the thermal stress of the coal body is enough to destroy the weaker structure, and the internal pore system of the coal body is reconstructed. The native cracks and new cracks inside the coal sample expand and develop at this stage. Hence strong AE signals are generated. In the subsequent heating stage of 15,000~20,000 s, the surface temperature of the coal sample continues to rise. More and more particles beyond the yield stress are inside the coal sample, so the destruction of pore structure and crack expansion are also increasing, the integrity of the coal body is seriously damaged, and the AE signal is further enhanced.

The cumulative count curve of AE is fitted to obtain a univariate linear regression curve with a slope of 5.316 and an apparent linear law, indicating that with the increase of temperature during the heating of the coal body, the AE signal continues to increase, and the level of AE count continues to increase.

As can be seen from Figure 3, with the progress of the experiment, the AE signal intensity shows a significantly enhanced trend. It has good consistency with the AE cumulative count diagram. In the initial heating stage of 0~5000 s, the coal body, due to the low temperature and the internal functional group of the coal body, failed to achieve the required activation energy. At this time, the redox reaction is weak, the coal body structure does not change significantly, and the AE energy is weak. In the continuous heating stage of 5000~15,000 s, the coal body has a higher temperature, the redox reaction of the coal body itself is more active, and the structure of the coal body is slightly damaged, so the AE signal energy is strong. In the subsequent heating stage of 15,000~20,000 s, the surface temperature of the coal sample continues to rise, the coal body obtains sufficient activation energy, and the internal structure is continuously decomposed and converted so that the coal structure is damaged. The AE energy continues to increase.

The cumulative energy curve of AE is fitted to obtain a univariate linear regression curve with a slope of 3.294 and an apparent linear law, indicating that with the increase of temperature during the heating of coal, the level of AE energy continues to increase, and the AE signal continues to increase.

In order to obtain the difference between the AE signal data at different temperatures, the AE counts and energy data of 5 min before and after 30 °C, 50 °C, 100 °C, 200 °C, and 300 °C are intercepted and plotted in Figures 4 and 5 below.

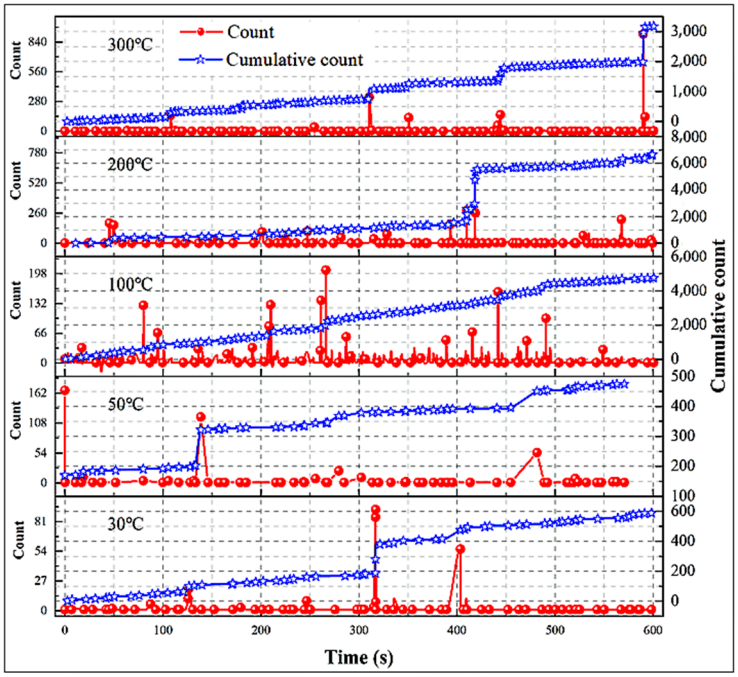

Figure 4. 600 s AE count of different temperature stages in the spontaneous combustion process of coal.

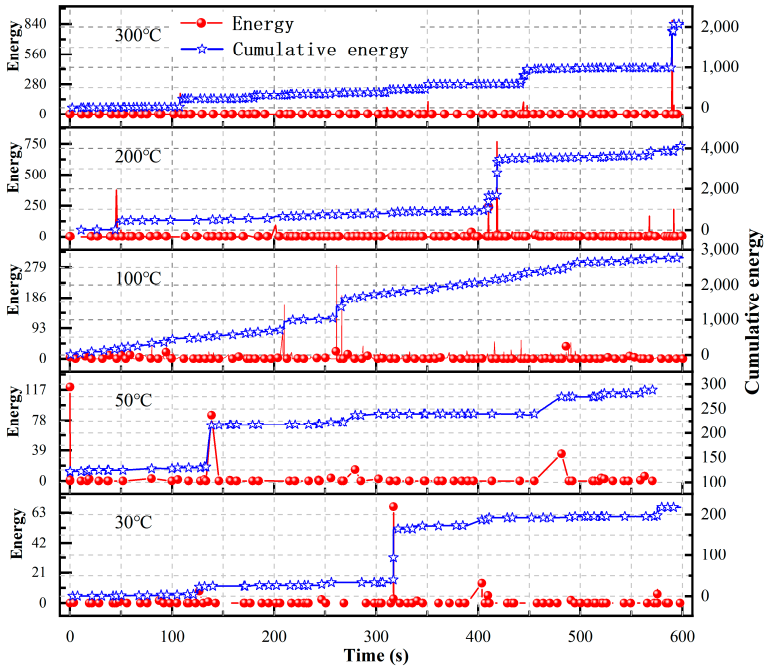

Figure 5. 600 s AE energy map of different temperature stages in the process of coal spontaneous combustion.

It can be seen from Figure 5 that there are fewer overall AE events at 30 °C and 50 °C. More AE signals at low counting points are generated, indicating that due to the lower temperature in the temperature band, the internal thermal expansion of the coal body is weaker, and the AE events are fewer. At 100 °C, there are more AE events, and a higher count of AE signals appear, indicating that in this temperature segment, a large amount of crystalline water disappears by heat evaporation of the coal body, resulting in more AE signals, and more pores have appeared on the surface of the coal sample, and the pore cracks are gradually increasing with the increase of temperature. At 200 °C, the internal

moisture of the coal body is tiny, and the thermal rupture phenomenon begins to appear. Hence, a robust AE signal appears, and the cracks on the surface of the coal sample expand and develop in this temperature segment. At 300 °C, the AE event of the coal body is more active, but the AE signal is also stronger, the thermal rupture phenomenon in the temperature band is completed, the thermal decomposition begins to appear, and the integrity of the coal sample at this time is seriously damaged, and it can be seen from the AE count data that the increase in temperature has a promoting effect on the generation of AE signals.

As shown in Figure 5, at 30 °C and 50 °C, the overall performance is relatively calm, a relatively small number of high-energy events occurred, and the overall energy amount value is low. At 100 °C, the coal body began to surge, the AE activity was active, and the AE signal at this time mainly came from the expansion and closure of the native fissure during the thermal expansion of the coal sample. At 200 °C, the AE activity is more active, with more high-energy events. The AE signal at this time mainly comes from the thermal expansion and rupture of the coal body, resulting in many pore fractures. At 300 °C, the AE activity is still relatively active. However, the intensity is slightly lower, indicating that the hot expansion material inside the coal body at this time has been completely expanded. A large number of cracks appear on the surface of the coal body, and the AE signal is mainly caused by the oxidative decomposition of the coal body by heat.

In order to explore the variation law of the maximum count and maximum energy in different temperature bands, the maximum values of the count and energy in the five temperature bands are selected and plotted, as shown in Figure 6 below.

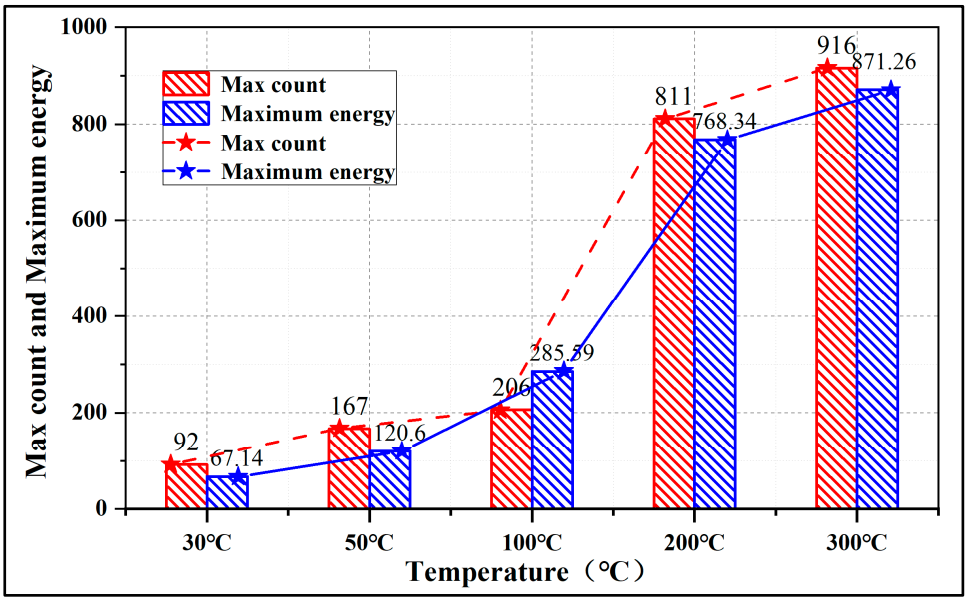

Figure 6. Maximum count and maximum energy of AE in different temperature segments.

Figure 6 is a graph of the maximum count and maximum energy change in the five temperature bands, and it can be seen from the figure that with the increase in temperature, the maximum count of AE shows a gradual increase trend, indicating that the temperature has a promoting effect on the AE signal. The maximum increase in the 30 °C–100 °C section is slight, indicating that the AE signal of the coal body is small and the change of the coal structure is small during this stage. In the temperature range of 100 °C to 200 °C, the maximum count of coal bodies increased significantly, indicating that during this time period, the rupture state of coal bodies changed, the AE signal was more active, and the internal structure of coal bodies changed greatly. There is still a slow growth trend in the maximum count of coal bodies at 300 °C, indicating that the coal body is in the same rupture state at 200 °C–300 °C. The maximum energy is in the temperature range of 30 °C to 100 °C. There is a slow growth trend, indicating that the coal structure changes little at

this stage. In the temperature range of 100 °C to 200 °C, the maximum energy growth of the coal body is large, indicating that in this temperature range, the rupture mode of the coal body changes so that the energy is greater. At 300 °C, the maximum energy of the coal body still increases compared with 200 °C, indicating that the structural evolution of the coal body is continuing.

3.2. Time-Frequency Analysis of AE Signals during Coal Spontaneous Combustion Heating

The measured data are analyzed using a fast Fourier transform (FFT), and the following is an introduction to the principle of FFT [34,35]:

$$x(k) = \sum_{n=0}^{N-1} x(n) e^{-2j\pi nk/N} \tag{1}$$

The inverse transformation is:

$$x(k) = \frac{1}{\mathrm{N}} \sum_{n=0}^{N-1} x(k) e^{2j\pi nk/N} \tag{2}$$

where: $x(k)$ is the kth value of the discrete spectrum, $k = 0, 1, ..., N-1$; $x(n)$ is the nth value of time domain sampling, $n = 0, 1, ..., N-1$.

The original waveform signals emitted by sound emissions from five different temperature bands during the heating process are extracted. Fast Fourier transforms (FFT) are performed to obtain a two-dimensional spectrogram.

The four small plots in the four typical power spectra of Figure 7 are interpreted for the four states. The main frequency of AE (peak frequency) corresponds to the maximum amplitude in the two-dimensional spectrogram. The main frequency and secondary frequency not in the same main peak is called a double peak, and the same main peak is called a single peak. When the frequency of the second frequency is higher than the main frequency, it is called high frequency, and when the frequency of the second frequency is lower than the main frequency, it is called low frequency. In this paper, eight AE events are selected around the five temperatures, and the probability of occurrence of each type of frequency is obtained by the fast Fourier transform, as shown in Table 2.

Table 2. Power spectrum probability table for different temperature types.

Waveform Type	Single Peak High Frequency	Single Peak Low Frequency	Bimodal High Frequency	Bimodal Low Frequency
30 °C	10%	30%	40%	20%
50 °C	10%	20%	70%	0%
100 °C	10%	20%	20%	50%
200 °C	10%	0%	60%	30%
300 °C	0%	10%	80%	10%

From Table 2 above, it can be seen that the number of occurrences of high bimodal frequency and bimodal low frequency measured in the experiment is more. The single peak high frequency and single peak low frequency are less. Fourier transform through MATLAB was used to obtain the main frequency amplitude of five temperatures. The AE signal at 30 °C–100 °C is mainly low frequency, the amplitude is slightly increased, and at 200 °C, it is mainly based on low frequency and high amplitude. At 300 °C, the AE signal is mainly based on high frequency and low amplitude. The difference between the main frequency and the amplitude category at different temperatures is large. It shows that with the increase of temperature, the probability of higher frequency main frequency AE signal will also increase, and there will be almost no high-frequency main frequency AE event before 50 °C, and when the temperature exceeds 50 °C, the high-frequency AE events

begin to appear. Thus, the AE frequency provides certain conditions for coal spontaneous combustion monitoring and early warning.

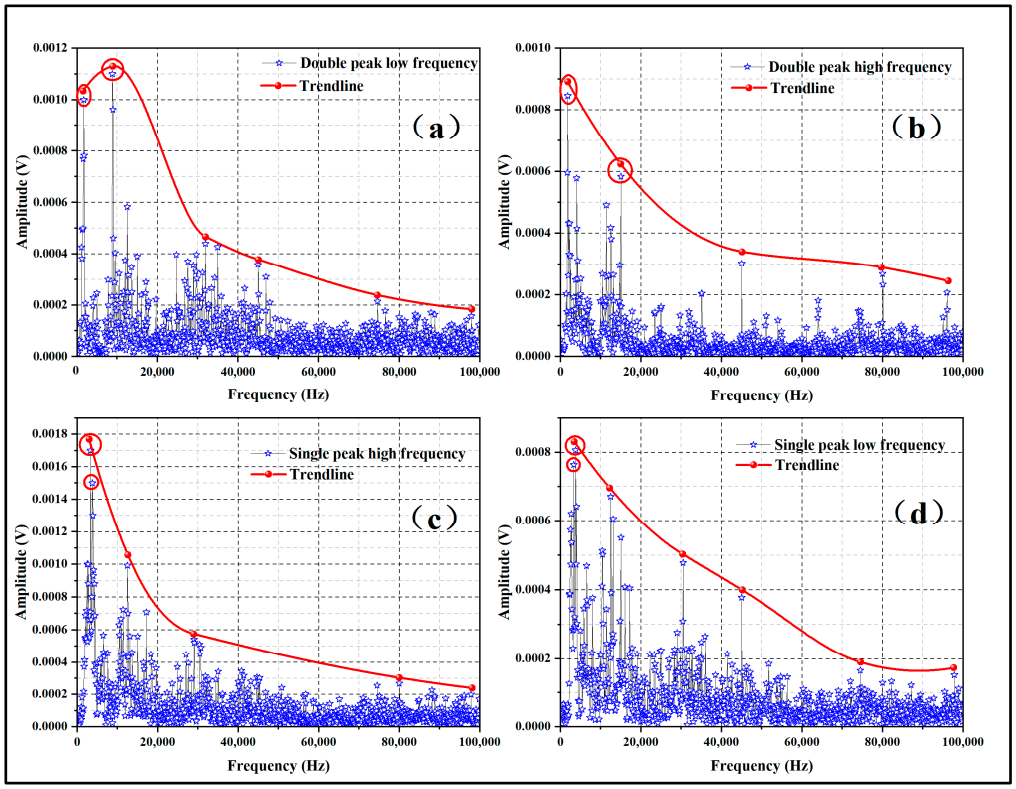

Figure 7. Spectrograms of four typical power articles. (**a**) double peak low frequency; (**b**) double peak high frequency; (**c**) single peak high frequency; (**d**) single peak low frequency.

The average frequency of the main frequency of the AE signal of five coal samples is calculated, and the average frequency fitting curve of coal at different temperatures is plotted, as shown in Figure 8. The fitting curve of the main frequency average frequency of coal at different temperatures shows that with the increase of temperature, the average frequency of the main frequency of AE gradually increases, so it can be known that the main frequency of AE shows a positive correlation with temperature, and this law can be used as the basis for judging the temperature change of the goaf area under the coal mine.

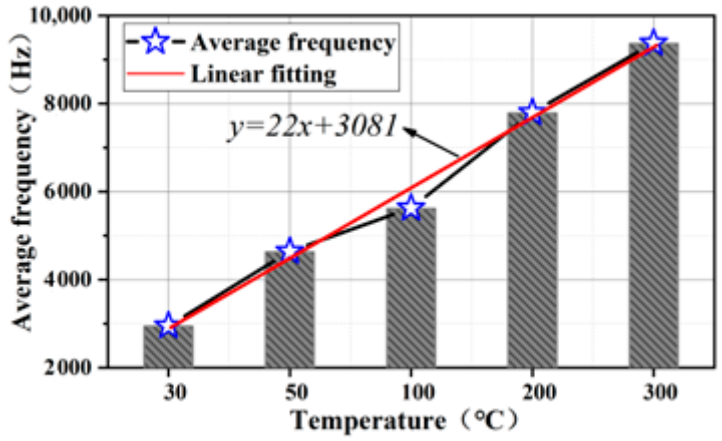

Figure 8. The average frequency of the main frequency of coal under different temperature conditions.

4. Study on the Fractal Law of Coal Spontaneous Combustion Heating Process

4.1. Fractal Law of Pore Structure of Coal Body after Treatment at Different Temperatures

In this paper, the fractal dimension "A = D − 3" is calculated by using the FHH model and capillary force. The nitrogen adsorption curve is divided into two parts at P/P0 = 0.5; the fractal dimension calculated from the P/P0 < 0.5 curve part is recorded as D2 as the fractal dimension of the pore surface. The fractal dimension calculated from the P/P0 > 0.5 curve part is the fractal dimension of the pore structure is recorded as D1. The fractal calculation of the coal samples treated at four different temperatures is performed, and the obtained data is plotted in Figure 9 below.

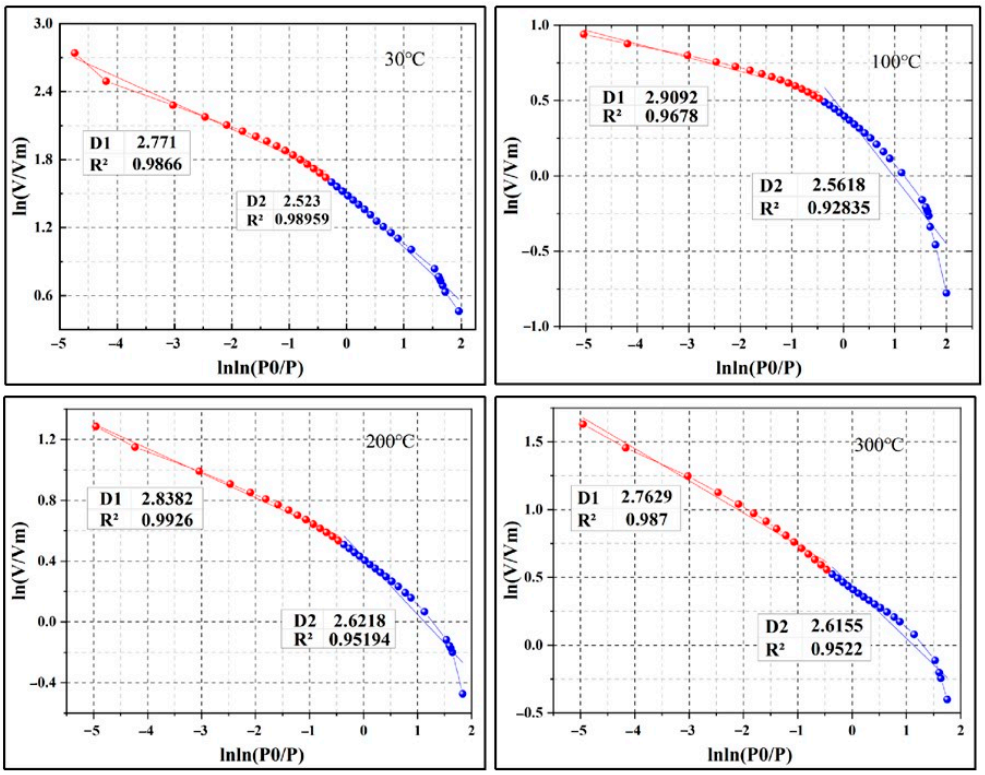

Figure 9. Fractal dimension fitting curve after different temperature treatments.

D1 and D2 are obtained from the fractal dimension fitting curve of Figure 9, where D1 is the fractal dimension of the high-pressure segment, that is, the fractal dimension of the pore structure. D2 is the fractal dimension of the low-pressure segment, that is, the fractal dimension of the pore surface. In Table 3, fractal dimensions of different pore sizes are obtained by different temperature treatments.

Table 3. Fractal dimensions after different temperature treatments.

	30 °C	100 °C	200 °C	300 °C
D1	2.771	2.909	2.838	2.763
D2	2.523	2.562	2.622	2.616

It can be seen from the table that with the increase of temperature, the fractal dimension of pore structures D1 and D2 are the same, in the temperature range from 30 °C to 100 °C; as the temperature rises due to thermal evaporation, the coal structure gradually becomes more complex, the pore structure continues to increase, and D1 increases. In the temperature section of 100~300 °C, the internal moisture of the coal body has been volatilized in large quantities, and the thermal expansion phenomenon of coal has begun to appear, resulting in the squeezing and closing of some pores and the reduction of D1. Coal

pore surface fractal dimension D2 generally showed an upward trend, indicating that the coal surface pore fracture structure tends to be complex. With the temperature of 30 °C to 200 °C, the surface moisture and volatile substances of the coal body are heated and evaporated so that the number of pores on the surface of the coal increases, and the coal surface structure is more complex. When the temperature reaches 200 °C, D2 shows a downward trend indicating that the coal surface structure tends to be flattened at this temperature. The surface part of the pore cracks is squeezed and closed due to heat expansion, resulting in a decrease in the complexity of the coal surface structure. D2 is reduced accordingly.

4.2. Fractal Law of Large-Scale Coal Spontaneous Combustion AE Count

4.2.1. Fractal Theory and the Determination of Phase Space Dimensions

In this paper, the associative dimension characteristics of AE counts are introduced, combined with the G-P algorithm [36], MATLAB software is used to calculate the bi-logarithmic relationship under different experimental conditions [37], and the count of AEs is used as the basic parameter to determine a series set with a capacity of n:

$$X = \{x_1, x_2, \ldots x_n\} \tag{3}$$

The first m number in Equation (3) constitutes the phase space (m < n) of the m dimension,

$$X_1 = \{x_1, x_2, \ldots x_m\} \tag{4}$$

The following data bits are sequentially extended by 1 to obtain N = n − m + 1 vector,

$$X_2 = \{x_2, x_3, \ldots x_{m+1}\}, X_3 = \{x_3, x_4, \ldots x_{m+2}\} \tag{5}$$

The corresponding associated dimensions are:

$$C(r(k)) = \frac{1}{N^2}\sum_{i=1}^{N}\sum_{i=1}^{N} h[r(k) - |X_i - X_j|] \tag{6}$$

where: h is the Riverside function; *r(k)* is a given scale function. Each determined scale *r(k)* corresponds to it. Each (lgr, lgC(r)) coordinate point is linearly fitted, and the slope after fitting is the associated dimension of the AE count. m is the phase space dimension, the size of m has a specific influence on the associated dimension, and the value of m is 1, 2, 3, 4, 5 ... 20. With the increase of m value, the correlation dimension gradually tends to be saturated and stable. At m = 10, the associative dimension gradually tends to saturate and stabilize, so the phase space dimension m = 10 is determined.

4.2.2. Determination of Fractal Features of AE Counts

According to the introduction of literature [38–46], when the scale coefficient $k \leq 0.1$, the fractal characteristics of the AE sequence are not prominent. This paper takes the scale factor $k > 0.1$ to calculate the associated dimension in the process of aqueous coal sample rupture. Moreover, the slope of the regression function is the associated fractal dimension. Figure 10 is a curve plot obtained by selecting 5 points with good lnr and lnC value conditions processed by MATLAB software, and after performing univariate linear regression analysis. It is found that the correlation coefficients R^2 of the AE counts of 30 °C, 100 °C, 200 °C, and 300 °C are 0.96, 0.97, 0.99, and 0.98, respectively, and the correlation coefficient R^2 is more significant than 0.90. The correlation between lnr and lnC is relatively high, indicating that the correlation between AE counts at different temperatures is high, and the AE count sequences of different temperatures during the spontaneous combustion of large-scale coals have obvious fractal characteristics.

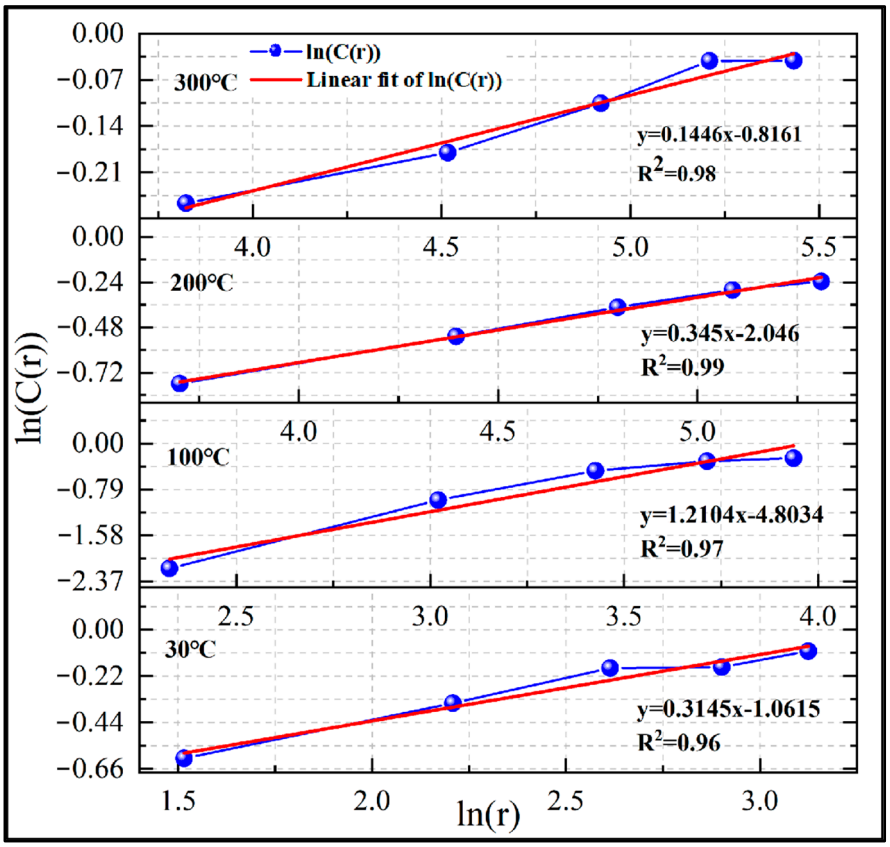

Figure 10. Fit curve plot of double logarithmic relationship at different temperatures.

4.2.3. Fractal Characteristics of AE Counting

According to the fractal characteristics of the AE count determined above, the fractal dimension change of the large-scale coal spontaneous combustion AE count is plotted, as shown in Figure 11.

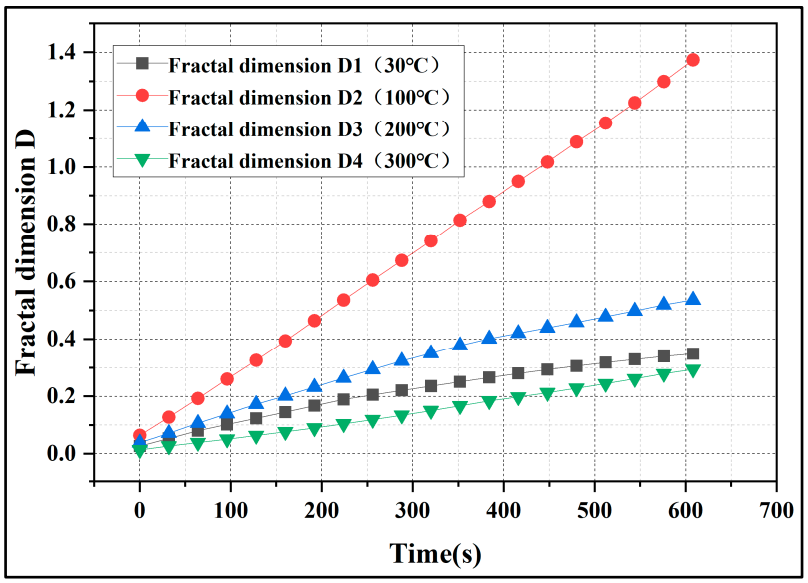

Figure 11. Fractal dimension change of AE counts at different temperatures.

The fitted slopes of the different fractal dimension change curves were 0.999, 0.987, 0.981, and 0.998, respectively. According to the fractal dimension change chart of the

AE count within 300 s before and after the temperature points of 30 °C, 100 °C, 200 °C, and 300 °C in the large-scale coal spontaneous combustion heating process, it can be seen that the fractal dimension of the sound emission count of the four temperature gradients continues to increase with the increase of time in the 300 s before and after the temperature, the linear law is very obvious, the slope is stable, and it is greater than 0.950, indicating that the AE events of the coal body continue to increase during the heating process, and the AE signal is continuously enhanced. The fractal dimension of the AE count at 30 °C increased from 0.0258 to 0.3487, the fractal dimension of AE at 100 °C increased from 0.0638 to 1.3735, the fractal dimension of the AE count at 200 °C increased from 0.0377 to 0.5630. The fractal dimension of AE at 300 °C increased from 0.0130 to 0.2937, indicating that the fractal dimension of the AE count was greatest at 100 °C and the smallest at 300 °C, showing a trend of first growing and then declining from 30 °C to 300 °C.

Figure 12 is the selection of m = 4, 8, 12, 16, 20 of the AE fractal dimensions with the temperature of the trend plot. The plot presents an inverted V-shaped feature; the fractal dimension of the AE count with the increase of temperature first shows an increase. Then it shows a downward trend; the m value is different, the change situation is the same, and the larger the m value, the greater the fractal dimension. According to the literature, the changing trend of fractal dimension can reflect the failure process of the coal body and the timing change of the AE signal. The larger the fractal dimension, the more disordered the AE event. Therefore, in the process of coal spontaneous combustion and heating of large-scale coal, the AE event of coal spontaneous combustion developed from orderly to disorderly with the increase of temperature and then from disorder to order. It further shows the increasing level of acoustic emission count and the increasing acoustic emission signal during the warming process of coal spontaneous combustion. The acoustic emission events show a change process from order to disorder and then from disorder to order.

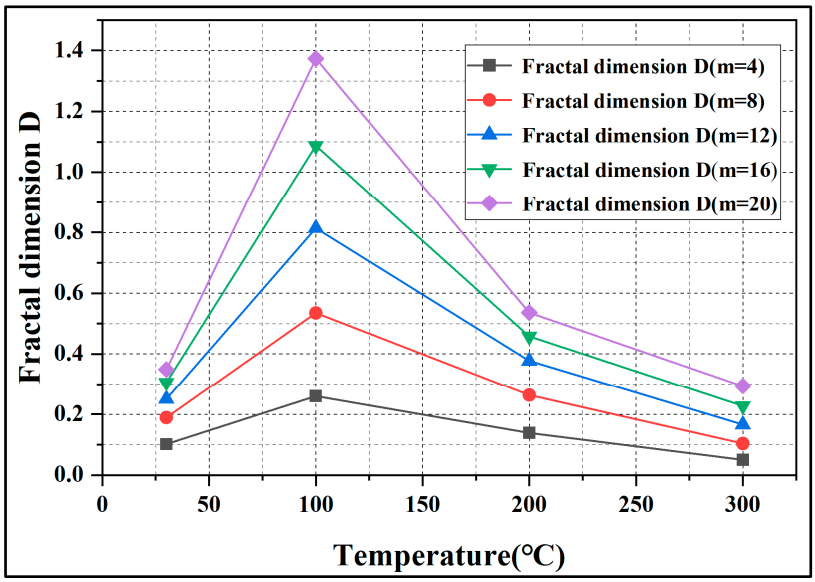

Figure 12. Variation of fractal dimension of AE counts with different m values.

The above trend of fractal dimension of AE count shows that there is a certain regularity in the sound emission count during the spontaneous combustion heating of coal. The fractal dimension level of the AE count near a specific temperature is continuously improved, which further indicates that the sound emission count level of the coal spontaneous combustion heating process is continuously enhanced, and the AE signal is continuously enhanced. The AE event shows a change process from order to disorder and then from disorder to order.

4.3. Discussion

In this paper, by constructing a large-scale AE test system, we tested the change law of the AE signal during the warming process of coal. The obtained data were Fourier transformed to systematically test the AE signal generated during the warming process of coal and comprehensively compare and analyze the intensity, energy scale, and timing characteristics of the AE signal, which showed a gradual increase as the experiment proceeded. At the beginning of the experiment, the coal did not obtain enough energy, and the thermal stress was not enough to destroy the coal itself, and only more small cracks were produced; at the middle of the experiment, the thermal stress of the coal itself was enough to destroy the weaker structure, and the internal pore system of the coal was reconstructed, and at this stage, the primary cracks and new cracks inside the coal sample expanded and developed so more strong acoustics. At the later stage of the experiment, the surface temperature of the coal sample was increasing, so the destruction of the pore structure and crack expansion were also increasing, and the integrity of the coal body was seriously damaged. This indicates that the AE signal can effectively respond to the damage and crack evolution of the coal body and can realize the monitoring and early warning of coal spontaneous combustion. The passive monitoring of AE, combined with the corresponding active detection of the fire source, can effectively improve the efficiency of coal spontaneous combustion monitoring and early warning and realize the joint detection of coal spontaneous combustion fire, which provides theoretical guidance for the subsequent research.

In order to study the AE signal to realize the monitoring and early warning of coal spontaneous combustion, this paper analyzes the time-frequency characteristics of the AE signal in the process of coal spontaneous combustion and the change law of the main frequency of the AE signal in the process of coal spontaneous combustion is obtained by Fourier transform calculation. In addition, the characteristic frequency spectrum is divided into four types, and the fitted curve of the main frequency average frequency of coal under different temperature conditions is analyzed and obtained, which can effectively reflect the phase change of the coal spontaneous combustion process by the AE signal. Chai and Ambrosio [47,48] studied the structural health detection of objects by the peak frequency and center of mass frequency of AE signal, and the research has been applied in nondestructive testing, welding, and microseismic, which can effectively respond to the changes of AE signals. Therefore, it is important to deeply explore the spectral characteristics of AE signal during coal spontaneous combustion through peak frequency and center-of-mass frequency to determine the correlation between temperature and AE signal during coal spontaneous combustion, and it is needed to further explore the correlation between damage rupture and AE signal during coal spontaneous combustion so as to realize the efficiency of coal spontaneous combustion monitoring and early warning.

The fractal dimension law of the pore structure of low-temperature nitrogen-adsorbed coal during the warming process and the fractal dimension law of AE counting the two fractal dimension laws are obvious; the fractal dimension law of the pore structure of low-temperature nitrogen-adsorbed coal is similar to the fractal dimension law of AE counting, and the two fractal dimension change trends are the same. In order to analyze the characteristics of pore structure changes during the warming process of coal synchronously, our team has characterized the pore structure changes at different temperatures by SEM experiments in the previous study. The integrity is good, and the pore structure is single under the room temperature condition (30 °C); after treatment at 100 °C, the integrity of the coal sample is slightly damaged, and the number of surface pores increases. At 200 °C, the integrity of the coal sample is damaged, and the number of surface pores increases. The integrity of the coal sample was damaged after treatment at 200 °C, and a large number of regional pore clusters appeared on the surface, and the pore size increased significantly compared with that at room temperature. At 300 °C, the integrity of the coal sample was severely damaged, and some of the fissures were connected with each other, and the connectivity was good. Based on this, the fractal dimension law of coal pore structure and

the fractal dimension law of AE counting were investigated by low-temperature nitrogen adsorption experiments. The results of the study showed that from 30 °C to 100 °C, the fractal dimension D1 of the pore structure of the coal body and the fractal dimension of the AE count showed a significant upward trend, combined with the analysis of the AE count and the cumulative count of AE, the coal body was heated and ruptured by heating during the heating process, and the nitrogen adsorption of the coal body continued to increase. From 100 °C to 300 °C, the fractal dimension D1 of the pore structure of the coal body and the fractal dimension of the AE count showed a downward trend, which was due to the thermal expansion phenomenon caused by the evaporation of a large amount of water in the coal body, resulting in the extrusion and closure of the pores of the coal body, and the growth rate of nitrogen adsorption decreased. Similarly, the fractal dimension D2 of the pore surface of the coal body has the same change trend at 30 °C–200 °C and 200 °C–300 °C, which further indicates that the pore structure of the coal body produces thermal rupture with the heating of the coal body. The thermal expansion phenomenon leads to the closure of some pores of the coal body. With the increase in temperature, the level of AE count continues to increase. The fractal dimension of the AE count rises first and then declines, indicating that with the increase in temperature, the AE signal continues to increase, and the AE signal shows a change law from order to disorder and then from disorder to order.

The experiment verifies the law that the pore structure of the coal body continues to generate and gradually increases during the heating process of the coal body. The fractal law of the low-temperature nitrogen adsorption curve and the fractal law of the AE count are analyzed, which further illustrates that the pore structure of the coal body in the process of heating up is the root cause of the AE signal of the coal body. The number of pores and the pore size of the coal body in spontaneous combustion and heating is increasing, which in turn leads to the continuous enhancement of the AE signal. Therefore, AE signals can be used for monitoring and early warning of coal spontaneous combustion.

5. Conclusions

1. With the increase in time and temperature, the count and energy of AE continue to increase, and the maximum count and maximum energy of AE continue to increase. The cumulative count of AE and the cumulative energy of AE continue to increase; it shows that the integrity of coal samples is destroyed during the heating process, the pore structure is constantly complex, the number of pores is increasing, the thermal damage rupture is increasing, and the AE signal released by the coal body is continuously enhanced.
2. The probability of the occurrence of high-frequency main frequency AE signals increases with the increase in temperature. The average frequency of the main frequency also increases. The main frequency of the acoustic transmission signal and its average frequency show a positive correlation with temperature; it shows that with the increase in temperature, the thermal damage of the coal body increases, and the AE signal continues to increase.
3. During the spontaneous combustion heating process of the coal body, with the increase of time and the increase of temperature, the fractal dimension of the low-temperature nitrogen adsorption curve and the fractal dimension of the AE count appear to rise first and then decline. It shows that due to the thermal expansion of the coal body in the process of heating up, the growth of the number of pores in the coal body rises first and then declines. The AE signal intensity of the coal body rises first and then declines, and the AE signal from order to disorder, from disorder to order, shows an increasing trend.
4. The law that the pore structure of the coal body is continuously generated and gradually enhanced during the heating process of the coal body further illustrated that the AE signal in the process of heating and heating of the coal body comes from the generation of the pore structure. The number of pores in the spontaneous combustion and heating process of the coal body continues to increase, and the

complexity increases, which in turn leads to the continuous enhancement of the AE signal. Therefore, the AE signal provides favorable conditions for monitoring and early warning of coal spontaneous combustion.

Author Contributions: Writing—original draft, J.Y., B.K. and L.S.; Writing—review & editing, Z.L. and W.L.; Formal analysis, X.P.; Supervision, Z.Z.; Data curation, L.J. All authors have read and agreed to the published version of the manuscript.

Funding: This research was jointly supported by the National Natural Science Foundation of China (51904172), the China Postdoctoral Science Foundation (2020M682209), the Natural Science Foundation of Shandong Province (ZR2019QEE041).

Data Availability Statement: The data used and/or analyzed during the current study are available from the corresponding author on reasonable request.

Conflicts of Interest: No potential conflict of interest was reported by the author(s).

References

1. Wu, L.X. The responsibility and development of coal under the double carbon target. *Coal Econ. Res.* **2021**, *41*, 1. [CrossRef]
2. Liu, C.; Xie, J.; Xin, L. A review of the theory and technology of spontaneous combustion prediction and forecasting of coal. *Min. Saf. Environ. Prot.* **2019**, *46*, 92–95+99.
3. Lu, W.; Wen, J.M.; Wang, D.; Zhang, W.R.; Hu, X.M.; Wu, H.; Kong, B. Study on gas transport characteristics of positive pressure beam tube system and its application to coal spontaneous combustion early warning. *J. Clean. Prod.* **2021**, *316*, 128342. [CrossRef]
4. Kong, B.; Li, J.H.; Lu, W.; Fu, W.; Song, H.Z.; Liu, J.F. Research on a Spontaneous Combustion Prevention System in Deep Mine: A Case Study of Dongtan Coal Mine. *Combust. Sci. Technol.* **2022**. [CrossRef]
5. Zhang, W.T.; Hou, Y.H.; Peng, D.H.; Fan, C. Distributed fiber optic temperature measurement and fire warning system in coal mines. In Proceedings of the 23rd National Conference on Coal Mine Automation and Informatization and the 5th China High Level Forum on Coal Mine Informatization and Automation, Beijing, China, 6–7 December 2013; pp. 74–80.
6. Zhang, X.H.; Liu, Q.; Zheng, X.Z.; Wang, W.F. Analysis of ZigBee-based wireless self-assembled temperature measurement system in mining area. *Coal Eng.* **2012**, *9*, 122–124.
7. Ganne, P.; Vervoort, A.; Wevers, M. Quantification of pre-peak brittle damage: Correlation between acoustic emission and observed micro-fracturing. *Int. J. Rock Mech. Min. Sci.* **2007**, *44*, 720–729. [CrossRef]
8. Ishida, T.; Kanagawa, T.; Kanaori, Y. Source distribution of acoustic emissions during an in-situ direct shear test: Implications for an analog model of seismogenic faulting in an inhomogeneous rock mass. *Eng. Geol.* **2010**, *110*, 66–76. [CrossRef]
9. Han, J.; Han, S.Z.; Ma, S.W.; Zhang, L.Y.; Cao, C. Study on acoustic emission characteristics of coal bodies of different strengths. *Chin. J. Undergr. Space Eng.* **2021**, *17*, 739–747.
10. Kong, B.; Zhuang, Z.D.; Zhang, X.Y.; Jia, S.; Lu, W.; Zhang, X.Y.; Zhang, W.R. A study on fractal characteristics of acoustic emission under multiple heating and loading damage conditions. *J. Appl. Geophys.* **2022**, *197*, 104532. [CrossRef]
11. Kong, B.; Zhong, J.H.; Hu, X.M.; Xin, L.; Zhang, B.; Zhang, X.L.; Zhuang, Z.D. Study on the change pattern of acoustic emission signal and generation mechanism during coal heating and combustion process. *Coal Sci. Technol.* **2023**, 1–8. [CrossRef]
12. Kong, B.; Zhu, S.X.; Zhang, W.R.; Sun, X.L.; Lu, W.; Ma, Y.K. Mechanical deterioration and thermal deformations of high-temperature-treated coal with evaluations by EMR. Geomechanics and Engineering. *Geomech. Eng.* **2023**, *32*, 233–244. [CrossRef]
13. Chen, C. Laboratory Study of Deformational Characteristics and Acoustic Emission Properties of Coal with Different Strengths under Uniaxial Compression. *Minerals* **2021**, *11*, 1070.
14. Zhang, R.; Liu, J.; Sa, Z.; Wang, Z.; Lu, S.; Wang, C. Experimental investigation on multi-fractal characteristics of acoustic emission of coal samples subjected to true triaxial loading-unloading. *Fractals* **2020**, *28*, 2050092. [CrossRef]
15. Wang, H.Y.; Wang, G.D.; Zhang, G.J.; Du, F.; Ma, J. Acoustic Emission Response Characteristics of Anthracitic Coal under Uniaxial Compression. *Shock. Vib.* **2020**, 1–12. [CrossRef]
16. Li, H.G.; Li, H.M.; Gao, B.B. Study on acoustic emission characteristics of rupture process of different coal-thick coal-rock assemblies. *J. Henan Polytech. Univ. (Nat. Sci. Ed.)* **2021**, *40*, 30–37.
17. Cai, Y.; Liu, D.; Yao, Y.; Li, J.; Liu, J. Fractal Characteristics of Coal Pores Based on Classic Geometry and Thermodynamics Models. *Acta Geol. Sin.* **2011**, *85*, 1150–1162. [CrossRef]
18. Guo, H.; Yuan, L.; Cheng, Y.; Wang, K.; Xu, C. Experimental investigation on coal pore and fracture characteristics based on fractal theory. *Powder Technol.* **2019**, *346*, 341–349. [CrossRef]
19. Li, Z.H.; Tian, H.; Niu, Y.; Wang, E.Y.; Zhang, X.; He, S.; Wang, F.Z.; Zheng, A.Q. Study on the acoustic and thermal response characteristics of coal samples with various prefabricated crack angles during loaded failure under uniaxial compression. *J. Appl. Geophys.* **2022**, *200*, 104618. [CrossRef]
20. Zhao, S.; Chen, X.J.; Li, X.J.; Qi, L.L.; Zhang, G.X. Experimental analysis of the effect of temperature on coal pore structure transformation. *Fuel* **2021**, *305*, 121613. [CrossRef]

21. Yi, M.H.; Cheng, Y.P.; Wang, C.H.; Wang, Z.Y.; Hu, B.; He, X.X. Effects of composition changes of coal treated with hydrochloric acid on pore structure and fractal characteristics. *Fuel* **2021**, *294*, 120506. [CrossRef]
22. Xu, C.P.; Li, H.; Lu, Y.; Liu, T.; Lu, J.X.; Shi, S.L.; Ye, Q.; Jia, Z.Z.; Wang, Z. Influence of microwave-assisted oxidant stimulation on pore structure and fractal characteristics of bituminous coal based on low-temperature nitrogen adsorption. *Fuel* **2022**, *327*, 125173. [CrossRef]
23. Jiang, L.; Chen, Z.; Ali, S.F. Thermal-hydro-chemical-mechanical alteration of coal pores in underground coal gasification. *Fuel* **2020**, *262*, 116543. [CrossRef]
24. Cheng, Q.Y.; Huang, B.X.; Li, Z.H. Research status of porosity and fracture of coal. *Coal Eng.* **2011**, *12*, 91–93.
25. Li, H.; Shi, S.L.; Lu, J.X.; Ye, Q.; Lu, Y.; Zhu, X.N. Pore structure and multifractal analysis of coal subjected to microwave heating. *Powder Technol.* **2019**, *346*, 97–108. [CrossRef]
26. Kong, B.; Wang, E.Y.; Li, Z.H.; Lu, W. Study on the feature of electromagnetic radiation under coal oxidation and temperature rise based on multifractal theory. *Fractals* **2019**, *27*, 1950038. [CrossRef]
27. Yang, S.Q. Study on the Evolution of Microstructure and Mechanical Response Law of Oil Shale under High Temperature Real-Time Action. Ph.D. Thesis, Taiyuan University of Technology, Taiyuan, China, 2021.
28. Li, J.H.; Xue, C.Z.; Han, Q. Study on the evolution characteristics of pore fractures in coal under different thermal fracture temperatures. *Coal Mine Saf.* **2020**, *51*, 22–25+29.
29. Lu, W.; Zhuang, Z.; Zhang, W.; Zhang, C.; Song, S.; Wang, R.; Kong, B. Study on the Pore and Crack Change Characteristics of Bituminous Coal and Anthracite after Different Temperature Gradient Baking. *Energy Fuels* **2021**, *35*, 19448–19463. [CrossRef]
30. Gan, Q.; Xu, J.; Peng, S.; Yan, F.; Wang, R.; Cai, G. Effects of heating temperature on pore structure evolution of briquette coals. *Fuel* **2021**, *296*, 120651. [CrossRef]
31. Gbadamosi, A.R.; Onifade, M.; Genc, B.; Rupprecht, S. Analysis of spontaneous combustion liability indices and coal recording standards/basis. *Int. J. Min. Sci. Technol.* **2020**, *30*, 723–736. [CrossRef]
32. Zhao, Y.S.; Meng, Q.R.; Kang, T.H. Micro-CT experimental technology and meso-investigation on thermal fracturing characteristics of granite. *Rock Mech. Eng.* **2008**, *27*, 28–34.
33. Kong, B.; Wang, E.; Li, Z.; Wang, X.; Chen, L.; Kong, X. Nonlinear characteristics of AEs during the deformation and fracture of sandstone subjected to thermal treatment. *Int. J. Rock Mech. Min. Sci.* **2016**, *90*, 43–52. [CrossRef]
34. Zhao, K.; Yang, D.X.; Gong, C.; Zhuo, Y.L.; Wang, X.J.; Zhong, W. Evaluation of internal microcrack evolution in red sandstone based on time–frequency domain characteristics of acoustic emission signals. *Constr. Build. Mater.* **2020**, *260*, 120435. [CrossRef]
35. Jia, X.N.; Jiang, Q.G.; He, M.C.; Ren, F.Q.; Du, S. Characteristic analysis of acoustic radio frequency spectroscopy of rhesus rock burst experiment in Laizhou granite. *J. Undergr. Space Eng.* **2018**, *14*, 51–57.
36. Song, X.X.; Tang, Y.G.; Li, W.; Wang, S.Q.; Yang, M.M. Fractal characteristics of structural coal adsorption holes in Zhongliang-shannan Mine. *J. China Coal Soc.* **2013**, *38*, 134–139.
37. Ji, H.G.; Wang, J.C.; Shan, X.Y.; Cai, M.F. Fractal characteristics of acoustic emission process of concrete materials and their application in fracture analysis. *Chin. J. Rock Mech. Eng.* **2001**, *6*, 801–804.
38. Tan, J.N.; Wang, B.; Feng, T.; Ning, Y.; Liu, B.B.; Zhao, F.J. acoustic emission characteristics of anchored sandstone under uniaxial compression and its connection with rock burst. *J. Cent. South Univ. (Nat. Sci. Ed.)* **2021**, *52*, 2828–2838.
39. Ding, X.; Xiao, X.C.; Lv, X.F.; Wu, D.; Wang, L.; Fan, Y.F. Study on fractal characteristics and acoustic emission law of coal body rupture. *J. China Coal Soc.* **2018**, *43*, 3080–3087.
40. Gao, B.; Li, H.; Li, H. Study on Acoustic Emission and Fractal Characteristics of Different Damage Types of Rock. *J. Undergr. Space Eng.* **2015**, *11*, 358–363.
41. Gao, B.B.; Li, H.G.; Li, L.; Wang, X.L.; Yu, S.J. acoustic emission and fractal characteristics of soft hard coals in the same group. *Chin. J. Rock Mech. Eng.* **2014**, *33*, 3498–3504.
42. Jin, P.J.; Wang, E.Y.; Song, D.Z. Study on Correlation of Acoustic Emission and Plastic Strain Based on Coal-rock Damage Theory. *Geomech. Eng.* **2017**, *12*, 627–637. [CrossRef]
43. Li, H.R.; Shen, R.X.; Qiao, Y.F.; He, M.C. acoustic emission signal characteristics and its critical slowing down phenomenon during the loading process of water-bearing sandstone. *J. Appl. Geophys.* **2021**, *194*, 104458. [CrossRef]
44. Yang, X.H.; Ren, T.; He, X.Q. Experimental study of coal burst risk prediction using fractal dimension analysis of acoustic emission spatial distribution. *J. Appl. Geophys.* **2020**, *177*, 104025. [CrossRef]
45. Wang, C.L.; Hou Xl Liao, Z.F.; Chen, Z.; Lu, Z.J. Experimental investigation of predicting coal failure using acoustic emission energy and load-unload response ratio theory. *J. Appl. Geophys.* **2019**, *161*, 76–83. [CrossRef]
46. Liu, K.; Ostadhassan, M. Multi-scale fractal analysis of pores in shale rocks. *J. Appl. Geophys.* **2017**, *140*, 1–10. [CrossRef]
47. Chai, M.Y.; Hou, X.L.; Zhang, Z.X.; Duan, Q. Identification and prediction of fatigue crack growth under different stress ratios using acoustic emission data. *Int. J. Fatigue* **2022**, *160*, 106860. [CrossRef]
48. Ambrosio, D.; Dessein, G.; Wagner, V.; Yahiaoui, M.; Paris, J.-Y.; Fazzini, M.; Cahuc, O. On the potential applications of acoustic emission in friction stir welding. *J. Manuf. Processes* **2022**, *75*, 461–475. [CrossRef]